TECNOLOGÍA
Acta Ciientífica Venezolana, 57 (4): 130-137, 2006

CARACTERIZACIÓN DE UNA ALEACIÓN COMERCIAL AA3003 POR RESISTIVIDAD ELÉCTRICA: VALIDEZ DE LA TEORÍA DE REACCIÓN

Luiggi Agreda, Ney José

GFM, Dpto. de Física, Escuela de Ciencias, Núcleo de Sucre, Universidad de Oriente,Apdo. Postal 299. Cumaná, Estado Sucre, Venezuela.

Recibido: 24-03-2004

RESUMEN. Hemos estudiado la cinética de transformación isotérmica que ocurre en una aleación comercial AA3003 en el rango de temperaturas comprendido entre 350 °C y 550 °C usando medidas de resistividad eléctrica. El propósito del mismo es dar explicación a la diversidad de valores de energía de activación reportados en la literatura cuando se utiliza la teoría cinética de reacción. La resistividad eléctrica muestra un decrecimiento monótono hasta alcanzar un plateau, siendo tal decrecimiento menor a medida que la temperatura de envejecimiento isotérmica decrece. Para las temperaturas de 350 °C y 550 °C, luego de ligeras variaciones al comienzo del envejecimiento, el comportamiento de la resistividad indica la precipitación de una única fase, mientras que a temperaturas intermedias parecieran coexistir dos fases. En este trabajo logramos demostrar que varios modelos obtenidos de la teoría de reacción nos permiten obtener un rango reducido de la fracción transformada donde los valores de la energía de activación corresponden al proceso de precipitación de fases ricas en Mn. **Palabras Claves:** Aleación AA3003, Modelos de Reacción, Cinética de Precipitación, Resistividad Eléctrica.

CHARACTERIZATION OF A COMMERCIAL AA3003 ALLOY BY ELECTRICAL RESISTIVITY: VALIDITY OF THE REACTION THEORY

ABSTRACT: We have studied the isothermal transformation kinetics of a commercial AA3003 alloy by means of electrical resistivity measurements at temperatures ranging between 350 °C and 550 °C, with the purpose of providing an explanation for the wide array of activation energy values reported in the literature. The electrical resistivity shows a monotonic decrease up to a plateau, this decrease being lower as the aging temperature diminishes. After slight variations at the onset of the aging, the behavior of the resistivity indicates the precipitation of one phase at 350°C and 550°C, while two phases seem to coexist at intermediate temperatures. We show that several reaction theory models permitted us to obtain a reduced range of the transformed fraction where the activation energy values correspond to the process of precipitation of Mn-rich phases. **Key Words**: AA3003 Alloy, Reaction Models, Precipitation Kinetics, Electrical Resistivity.

INTRODUCTION

The characterization of phase transformation kinetics occurring in the solid state is a theme of great importance for both scientists and materials engineers, since it permits to visualize the physical and chemical mechanisms that explain not only properties of basic interest but also questions of industrial relevance.

Many theories have formally attempted to explain the changes of phases occurring in a material, the statistical theory of Binder et al.[1,16], based on clustering by coagulation and atomic evaporation, being the most elaborated. Similarly, Cahn[4] and Hillert[11], have proposed a classical approach to study the free energy variations associated with phase changes as a valid alternative to characterize a dynamic system. Bypassing the complications of these sophisticated theories, we[14] present a simplified version of the microscopic cluster theory, based on the main tenets of the Nucleation and Growth theory, thus rendering the problem of having to provide as many equations as atoms are diffused in the search of equilibrium to one of providing only as many equations as phases coexist in the process. Although our numerical results explain the two-phase transformations studied, no analytical solution was possible. We also propose a macroscopic version of the reaction theory as applied to multiphase reactions by considering the possible transformation paths. In all cases the problem is reduced to a differential equation or to a system of differential equations that tries to characterize the evolution of the transformation kinetics by involving as few parameters as possible.

The literature has been very precise in the use of reaction models to determine the characteristic criteria of the theory of transformation; however, such criteria are rather characteristic of the models but not of the kinetics, since each reports very disparate results; that is why the present work purports to ascertain the range of validity for each of these models in the case of isothermal data obtained by electrical resistivity in a commercial 3003 alloy.

THEORETICAL ASPECTS

The differential equation for the study of isothermal transformation kinetics involves the transformed fraction Y, the reaction constant K, and the kinetic or conversion functions G. Independence is assumed between K and G, K being a function of the temperature and G a function of Y, which allows us to write the simplified kinetics equation as:

$$\frac{dY}{dt} = K(T)G(Y) \qquad (1)$$

An integral form of Eq. (1) is written as

$$g(Y) = \int_0^Y \frac{dY}{G(Y)} = \int_0^t K(T)dt \qquad (2)$$

Several empirical reaction models have attempted to reproduce the kinetics of transformation by defining G(Y). Table I summarizes the models most widely used in the literature.[17,6]

We must also point out that in the case of the Johnson-Mehl-Avrami [5] model, P is associated with the coefficient of impingement, whereas N is a coefficient associated with the

geometry of the precipitates. P = 0 leads to the Johnson-Mehl[5] equation, whereas P = 1 reproduces the Austin-Rickett, AR, equation.[5]

Notice also that first- and second- order chemical kinetics are obtained from this model for the particular case of N = 1. In the case of Fuyita[7] and Damask *et al.*,[6] P is associated with the critical size of the precipitates formed by a process of nucleation and growth.

As Y is known experimentally as a function of time, the model parameters and the reaction constant K can be determined by nonlinear regression. For thermally activated processes, the reaction constant K follows an Arrhenius relation. (See Flynn[7] for a study of the equations showing the dependence of K on temperature),

$$K(T) = K_0 \exp\left(-\frac{Q}{RT}\right) \qquad (3)$$

where the pre-exponential factor K_0 and the activation energy of the process Q are characteristic parameters of the transformation. As K is experimentally known as a function of the temperature, ln K vs 1/T can be plotted and these parameters determined: The problem arises because each reaction model presents a different analytical form, and thus each of them will generate values that differ from such parameters, which will produce ambiguity in the results presented in the literature. The ambiguity so manifested has led many researches to focus their research on the so called isotransformation or isoconversion models.[17,2]

EXPERIMENTAL ASPECTS

The AA3003 alloy under study presents a wt. % composition of 1.1 Mn, 0.67 Fe, 0.28 Si, 0.1 Cu, 0.01 Ti, 0.005 Zr, 0.004 Mg, and balance aluminum. The samples were homogenized during 24 hours at 600 °C, quenched in an aqueous solution kept at 0 °C and then subjected to isothermal aging at 350, 400, 450, 500, and 550 °C.

The resistivity was measured by means of a Sigmatest D 2.068, which is a microprocessor controlled to measure the conductivity of nonmagnetic materials in the range of 0.5 to 65 MS/m (1 to 112 % IACS) with an absolute precision of ±1 % of the measured value. This allows us to access electric resistivity values in the range of 1.54 to 200 μΩ cm.

The samples used were 1-mm thick square sheets measuring 20 x 20mm^2. All the measurements were conducted at 20 °C, temperature at which the transition elements, or main alloying elements in the 3003 alloy, show little diffusivity in aluminum. To guarantee the reproducibility of the experience, homogenized samples with an initial value of 23.75 MS/m ± 1 % were selected. The isothermal aging was conducted in salt baths controlled at ± 2 °C.

RESULTS

Fig. 1 shows our experimental results. In it we have drawn the electrical resistivity ρ in function of the aging time at 350 °C, 400 °C, 450 °C, 500 °C, and 550 °C. We noticed a monotonic decrease with slight fluctuations in each case, fluctuations which occur mainly during the first stages of aging and which are associated to the particular precipitation of one or more alloying elements. This is more noticeable in the case of aging at 350 °C, where the Si precipitation elicits such fluctuations. At other temperatures the Si precipitates so quickly that its effect is masked by the early precipitation of Mn, whose effects at the electrical resistivity level are more important. There is a tendency for a change in the slope of the Á(t) curves to appear at intermediate aging temperatures (350 °C < T < 550 °C), a phenomenon which is associated to the structural phase changes, and the first part of which corresponds, according to previous studies,[5,6] to a rich Si-Fe metastable phase, and the second to the equilibrium phase Al_6(Mn,Fe). As the aging temperature becomes greater, the final resistivity plateau is less important on account of the increase of the solubility limit with the temperature, which results in a reduction of precipitable atoms.

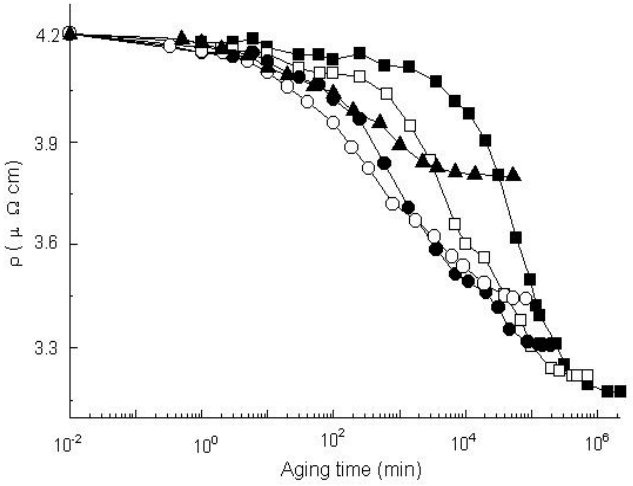

Figure 1. Electrical resistivity of an AA3003 commercial alloy versus aging time at different aging temperatures. ■ T = 350 ºC □ T =400 ºC ● T= 450 ºC ○ T = 500 ºC ▲ T = 550 ºC

The transformed fraction Y(t) is obtained from Fig. 1 using the relation,

$$Y(t) = \frac{\rho(0) - \rho(t)}{\rho(0) - \rho(\infty)} \qquad (4)$$

where, for a given temperature, $\rho(0)$ represents the resistivity before precipitation; ρ(t), the resistivity measured during precipitation at time t after aging starts; and $\rho(\infty)$ the resistivity measured at an aging time sufficiently long to guarantee no further variations of resistivity. Figure 2 reflects the precipitated fraction Y in function of the aging time at the temperatures noted above. The former analysis is thus confirmed, emphasizing the diffusive character of the process of transformation, reflected in the fact that the kinetics becomes much faster as the aging temperature gets higher.

Once Y(t) was known, we proceeded to evaluate the activation energy according to the models in Table I. The traditional fashion to perform this evaluation is a nonlinear regression that makes it possible to obtain the best

parameters to adjust the experimental data to such models; however, the best parameters only guarantee an average adjustment throughout the complete kinetics, thus resulting in each model generating different results.

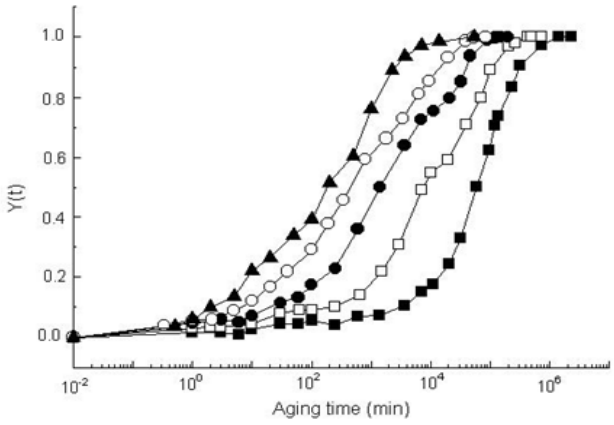

Figure 2. Transformed fraction versus aging time, deduced from figure 1. Same notation as in Figure 1.

To check the validity of the models proposed we used the integral form of our reaction equation and determined, according to Eq. (2) and plotting from graphic

$\frac{g(Y)}{t}$ versus t or $\frac{g(Y)}{t}$ vs Y, the region where K remains constant. From the values thus obtained and from the graphic of ln K versus 1/T we determined the value of the apparent activation energy Q for the process being considered as well as the t or Y range where such constancy is maintained.

Application to Reaction Models Defined by Power Laws

Table I. Reaction Models

n	Reaction Models	G(Y)	g(Y) = Kt
1	Power Law[17]	$NY^{\frac{N-1}{N}}$	$Y^{\frac{1}{N}}$
2	One-dimensional Diffusion[17]	$\frac{1}{2}Y^{-1}$	Y^2
3	Three-dimensional Diffusion[17]	$2(1-Y)^{\frac{2}{3}}\left[1-(1-Y)^{\frac{1}{3}}\right]^{-1}$	$\left[1-(1-Y)^{\frac{1}{3}}\right]^2$
4	Chemical Kinetics of the P-Order[3]	$(1-Y)^P$	$-\ln(1-Y)$ P=1 $(1-Y)^{-1}$ P=2
5	Johnson-Mehl-Avrami[5]	$N(1-Y)^{P+1}\left[-\ln(1-Y)\right]^{\frac{N-1}{N}}$	$\left[\ln\frac{1}{1-Y}\right]^{\frac{1}{N}}$ P=0 $\left[\frac{1}{1-Y}\right]^{\frac{1}{N}}$ P=1
6	Fujita-Damask[6,8]	$\frac{2(1-Y)}{P}\sqrt{1-(1-Y)^P}$	$\frac{1}{2}\ln\frac{\sqrt{1-(1-Y)^P}+1}{\sqrt{1-(1-Y)^P}-1}$ $\cosh^{-1}\left[\frac{1}{(1-Y)^{\frac{P}{2}}}\right]$

Under this denomination we assemble all the models whose reaction function is an integer or otherwise power of the transformed fraction Y, as shown in Table I. In general, the studies are undertaken for powers N = 2, 3, and 4. In our case N was left as a free parameter with the purpose of obtaining the value of N that would guarantee K's constancy. In this application we also included the function corresponding to the one-dimensional diffusion, which is a power function with N = 1/2. Figs. 3a -3e show our K results in function of the transformed fraction Y for each temperature and for different values of N. In these figures we drew a straight line in the regions where K remained constant, thus allowing ourselves to set the values of K and N, as well as the constant range for K.

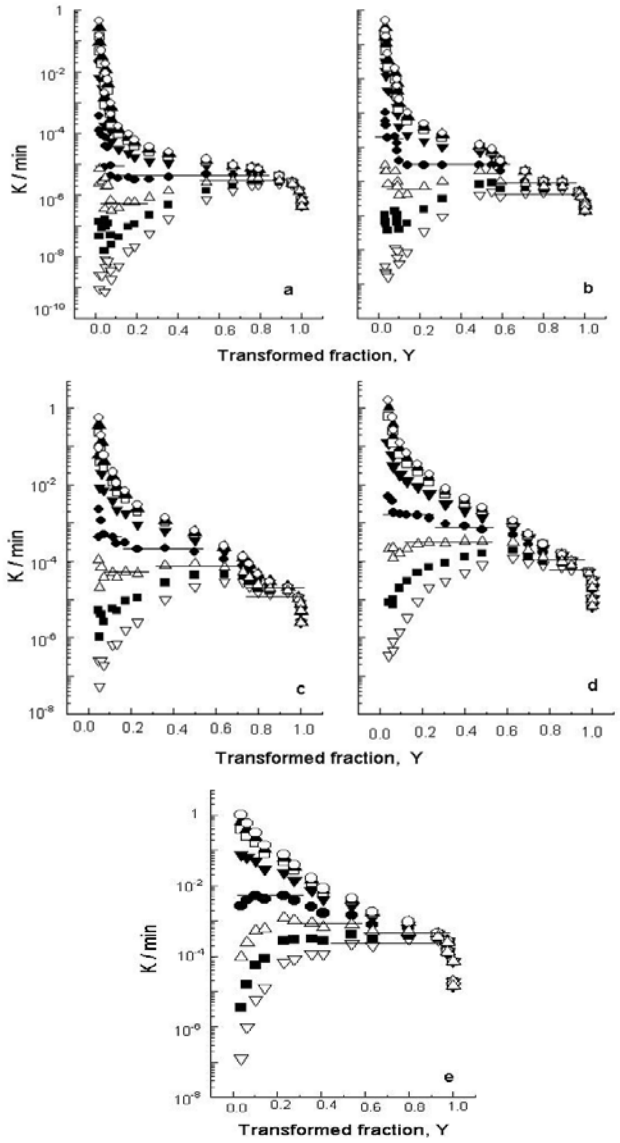

Figure 3. Reaction constant K versus the transformed fraction at different aging temperatures and different N values for a power law reaction model
3.a T = 350 °C. 3.b T = 400 °C. 3.c T = 450 °C. 3.d T = 500 °C 3.e T = 550 °C.
▽ N = 1/5 ■ N = 1/4 △ N = 1/3 ● N = 1/2 ▼ N = 1 □ N = 2 ▲ N = 3 ○ N = 5

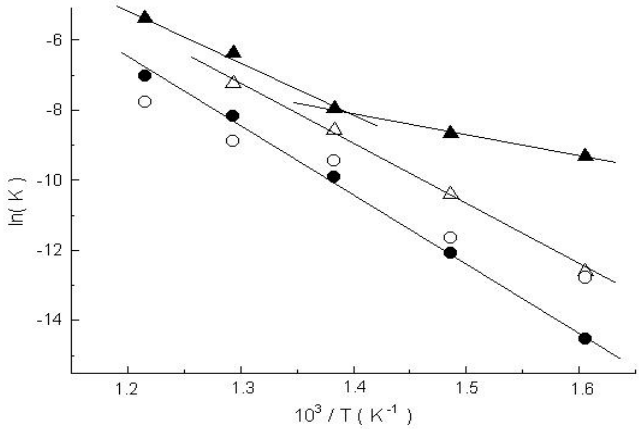

Figure 4. Natural logarithm of K versus the temperature inverse for the power law reaction model. ○ N = 1/3 for low Y values ● N = 1/3 for high Y values ▲ N = 1/2 for low Y values △ N = 1/2 for intermediate Y values.

From the analysis of these graphics we can identify the ranges of Y at each temperature where K remains constant. The values of N showing these constancy ranges at all temperatures are N = 1/3 and N =1/2, although a somewhat constant range can be observed for values of N = 1/5 at high Y values and temperatures over 400 °C. Unfortunately, the natural logarithms of these K values do not align themselves with the temperature inverse, thus preventing the application of the Arrhenius relation. Figure 4 shows the natural logarithm of K versus Y for N = 1/2 and N = 1/3. Depending on the constancy range of Y, different behaviors are identified for each N. For N = 1/2, during the first stages of precipitation (Y < 0.1) there occurs a process at temperatures below 450 °C with an activation energy of (51 ± 4) kJ/mol, whereas for temperatures above 450 °C the process thus engaged involves an energy of (128 ± 2) kJ/mol. A wide region of constancy of Y at 350 °C (0.07 < Y < 0.85) is identified in the intermediate stages of the transformation. This region diminishes as the aging temperature increases, until it disappears at 550 °C. A sole process whose activation energy is (145 ± 4) kJ/mol is reported in this range.

For N =1/3, a low Y range is obtained (0.1 < Y < 0.3) where the points do not align themselves with the inverse of the temperature, preventing the application of the natural logarithm of Eq. (3), whereas for Y values at the end of the transformation a process is identified that is common at all temperatures and whose activation energy is (162 ± 5) kJ/mol.

Application to the Three-dimensional Diffusion Model

Item 3 of Table I shows the mathematical relation defining this model. Fig. 5 shows the Y ranges where K remains constant at different aging temperatures. A constant K sequence for low Y values (Y < 0.25) at T < 550 °C, some isolated constant K values for intermediate Y values, and a new sequence for Y > 0.7 are observed. The graphic of the natural logarithm of K as a function of the temperature inverse is presented in Fig. 6, identifying for Y < 0.25 a process whose activation energy is (161 ± 3) kJ/mol, whereas there are two processes for high values of Y, one for T < 450 °C, the Q value of which is 48.2 kJ/mol, and another for high Ts with an energy of (156 ± 12) kJ/mol. In both cases the values obtained for high temperatures are indicative of a precipitation process controlled by Mn diffusion but slowed down by the presence of other alloying agents, mainly Si and Fe, coinciding with the diffusion corresponding to the precipitation of the $Al_6(Mn,Fe)$ phase.

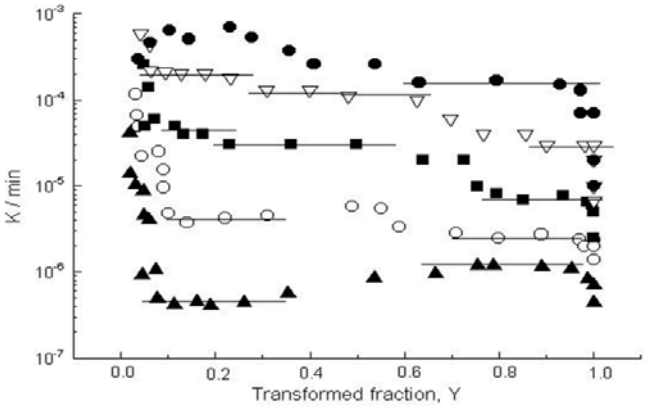

Figure 5. Reaction constant K versus the transformed fraction for the three-dimensional diffusion reaction model, at different aging temperatures. ▲ T = 350 °C ○ T = 400 °C ■ T = 450 °C ▽ T = 500 °C ● T = 550 °C.

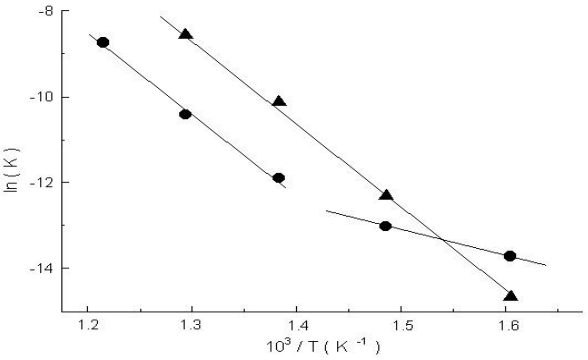

Figure 6. Natural logarithm of K versus the temperature inverse for the three-dimensional diffusion reaction model. ▲ Low Y values ● High Y values.

Application to reaction models defined by chemical kinetics of the order of 1 and 2

Figures 7a and 7b show the variation of the reaction constant with the transformed fraction for these models. For chemical kinetics of the first-order (Fig. 7a) K shows, for all aging temperatures, a decrease featuring Y constancy ranges that tend to become smaller as the aging temperature increases. The validity of this model is checked in Fig. 8 by the application of Eq. (2) for high values. Two processes are identified in this figure, an activation energy of (60 ± 7) kJ/mol corresponding to the process occurring at T < 450 °C and a value of Q reaching (150 ± 13) kJ/mol corresponding to the processes at higher temperatures.

As for second-order chemical kinetics, shown in Fig. 7b, the functional dependency of K on the T inverse is similar to that of first-order kinetics, the Y range where K remains constant being quite wide for T = 350 °C but reduced for other aging temperatures. Again, Fig. 8, for high Y values shows the occurrence of different processes of transformation, one for T < 450 °C, whose activation energy is 39 kJ/mol, and another for higher temperatures with an energy reaching (152 ± 4) kJ/mol.

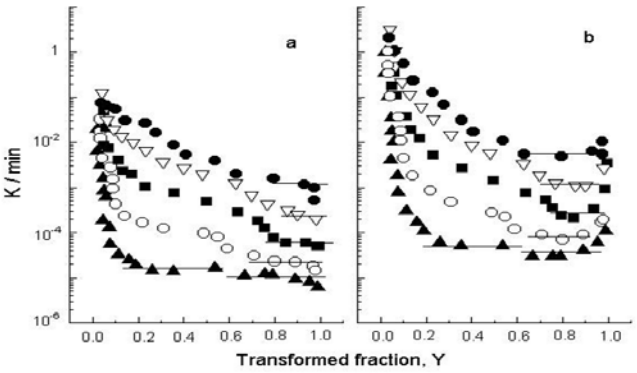

Figure 7. Reaction constant K versus the transformed fraction for the chemical kinetics reaction model, at different aging temperatures. 7.a First-order 7.b Second-order. ▲ T = 350 °C ○ T = 400 °C ■ T = 450 °C ▽ T = 500 °C ● T = 550 °C.

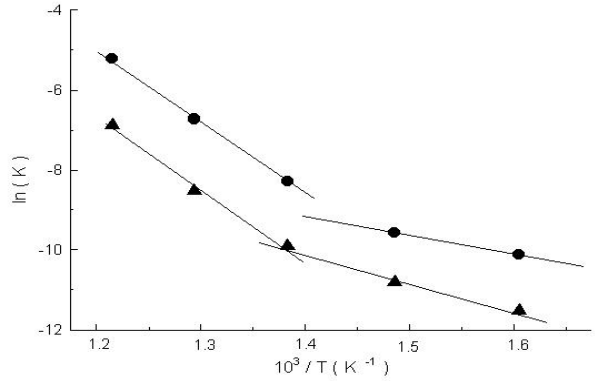

Figure 8. Natural logarithm of K versus the temperature inverse for the chemical kinetic reaction model, for high Y values. ▲ P = 1 ● P = 2.

Application to reaction models of the Johnson-Mehl-Avrami type

Our results for the JMA model with P = 0 for different aging temperatures are presented in Figs. 9a and 9e. We notice that the plotted K function changes from a decreasing aspect of N values close to 1 to an increasing aspect of N values close to 0. Obviously, the increasing-decreasing transition generates a region where K remains constant. In each of these figures it is possible to ascertain that for values of N = 1/3 and N = 1/2 there are regions that satisfy the constancy condition of K.

In Fig. 10 we draw an Arrhenius diagram to determine such energy. For N = 1/3 it is evident that for low values of Y, though there are constant regions of K, these regions are not aligned; whereas for intermediate values of Y (0.4 < Y < 0.8) there is no K constancy region at 350 °C. The process that occurs at the remaining temperatures is characterized by an activation energy of (112 ± 8) kJ/mol. For N = 1/2 we find different processes at low and high Ys. With the exception of the point at 550 ºC, the value of Q at low Ys corresponds to (157 ± 12) kJ/mol, whereas for values of Y >0.7 two processes are clearly distinguished: For T < 450 °C, a process whose activation energy is (68 ± 4) kJ/mol is identified, while for T > 450 °C the energy is (155 ± 4) kJ/mol. Again, the presence of the $Al_6(Mn,Fe)$ phase for temperatures greater than 350 °C is confirmed by the magnitude of Q.

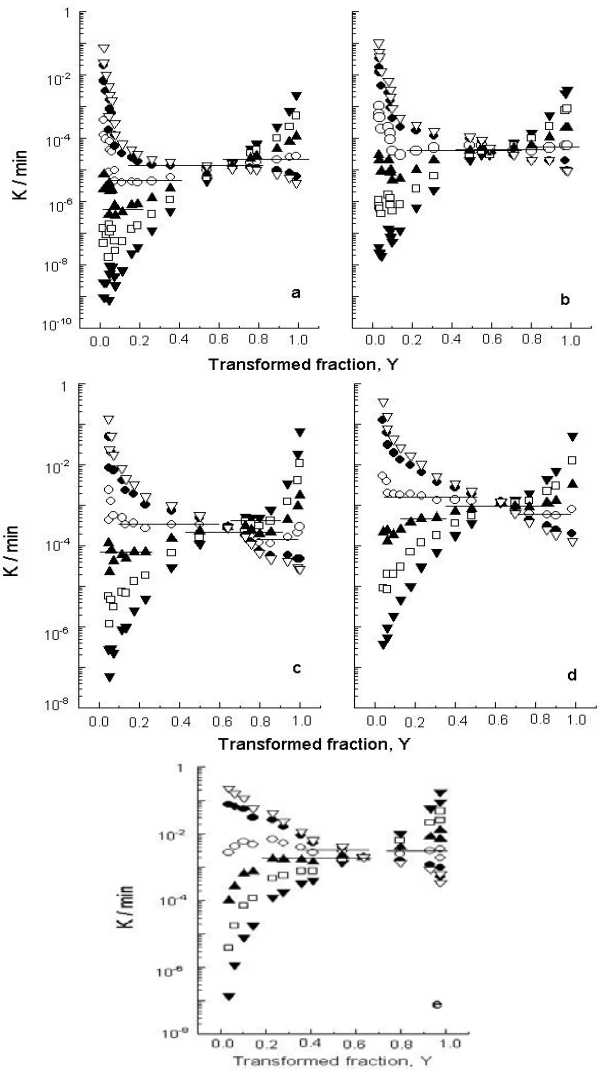

Figure 9. Reaction constant K versus the transformed fraction at different aging temperatures and different N values for the JMA (P = 0) reaction model.
9.a T = 350 °C. 9.b T = 400 °C. 9.c T = 450 °C. 9.d T = 500 °C 9.e T = 550 °C.
▼ N = 1/5 □ N = 1/4 ▲ N = 1/3 ○ N = 1/2 ● N = 1 ▽ N = 3/2.

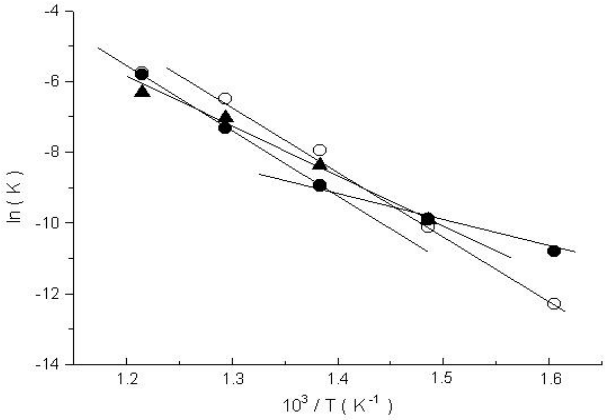

Figure 10. Natural logarithm of K versus the temperature inverse for the JMA (P = 0) reaction model. ▲ N = 1/3 for

intermediate Y values ○ N = 1/2 for low Y values ● N = 1/2 for high Y values.

It is important to point out that for this model the exponent N = 1/2 corresponds to a controlled diffusion growth resulting in the thickening of large disc-shaped particles.[9]

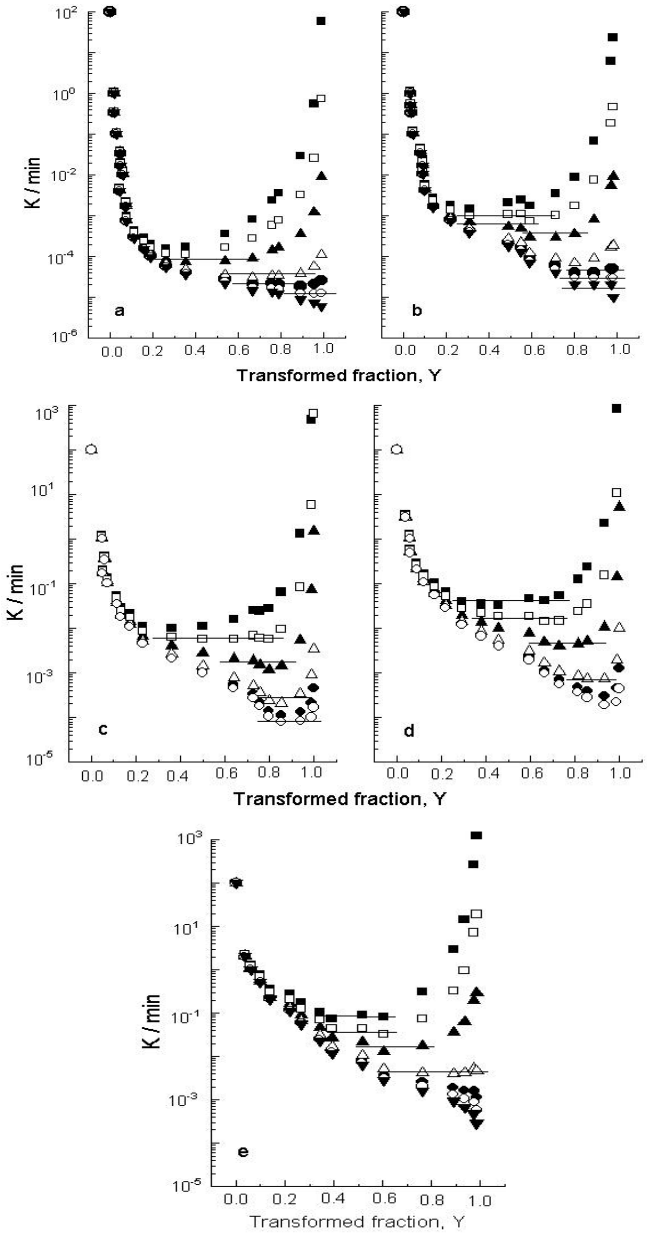

Figure 11. Reaction constant K versus the transformed fraction at different aging temperatures and different N values for the JMA (P = 1) reaction model.

11.a T = 350 °C. 11.b T = 400 °C. 11.c T = 450 °C. 11.d T = 500 °C 11.e T = 550 °C. ■ N = 1/4 □ N = 1/3 ▲ N = 1/2 △ N = 1 ○ N = 3.

The results for the case of P = 1, corresponding to the Austin-Rickett model, are shown in Figs. 11a - 11e. The figures show a decreasing dependency of K on low Ys, a sort of plateau, and then a curvature change tending to higher values of Y. This behavior permits to define different regions where K remains constant at each temperature. The N values that allow the sequential application of the natural logarithm of Eq. (3) are: 1/3, 1/2, and 1, respectively. Figure 12 plots the natural logarithm of K vs the temperature inverse for these values of N. For N = 1/3 and intermediate Y values (0.35 < Y < 0.7) a single process with an activation energy of (96 ± 4) kJ/mol is predicted at high temperatures. For N = 1/2 and Y values ranging from 0.6 to 0.8, a sole process with an activation energy of (111 ± 5) kJ/mol appears to insinuate itself, except at 350 °C, where Y ranges between 0.25 and 0.65; whereas for N =1, two processes are identified for a high Y range (0.6 < Y < 0.95): one at temperatures below 450 °C, with an activation energy of (66 ± 4) kJ/mol, and another above 450 °C, with an activation energy of (146 ± 22) kJ/mol.

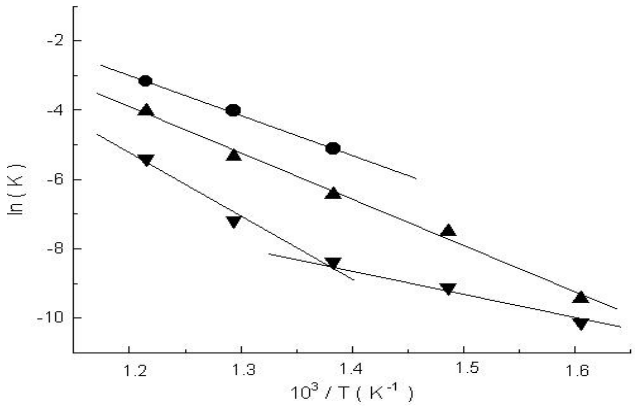

Figure 12. Natural logarithm of K versus the temperature inverse for the JMA (P = 1) reaction model. ● N = 1/3 for intermediate Y values ▲ N = 1/2 for intermediate Y values ▼ N = 1 for high Y values.

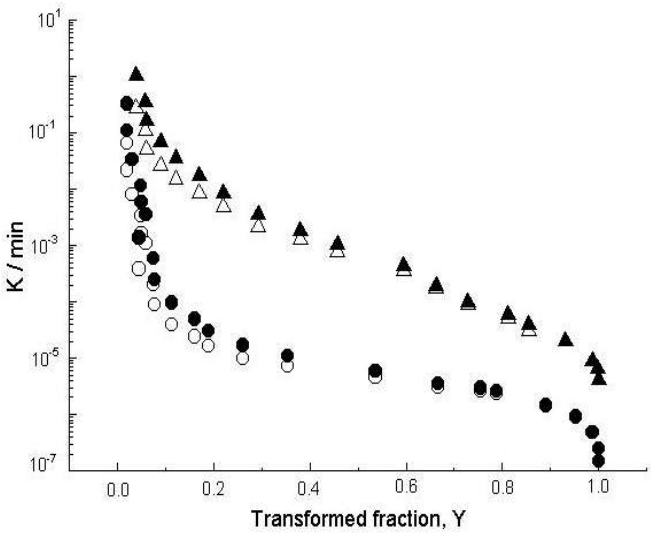

Figure 13. Reaction constant K versus the transformed fraction at different aging temperatures for the Fujita-Damask reaction model. Circles T = 350 °C. Triangles T = 500 °C. ● P = 100 ○ P = 1 ▲ P = 100 △ P = 1.

Application to the Fujita-Damask model

Physically, the first solution proposed by the Fujita-Damask kinetic equation, appearing in Table I, though mathematically correct for this model, does not lead to realistic results on account of the Y variation. Resorting to the solution proposed by Damask et al.[6] we have checked the solution with our data, obtaining a violent decrease of

K for low Ys and for all aging temperatures, and a violent K increase for all values of Y in the neighborhood of 1; whereas for intermediate Ys a slow K decrease appears at 350 °C, intensifying itself at higher temperatures. Figure 13 shows these results for 350 °C and 500 °C and for values of P = 1 and 100. It is obvious that the value of P = 1 presupposes a transformation where there is no nucleation and that bears no physical sense within the premises defining the Damask et al. model.[6] The fact that K is not constant demonstrates that the kinetics of the AA3003 alloy obtained by resistivity at the aging temperatures considered do not follow the premises of the Fujita-Damask model.

DISCUSSION

In the present discussion we will keep in mind the following basic facts: 1. The energy of diffusion of Mn in Al is 219 kJ/mol.[9] 2. The energy of formation of the Al_6Mn phase in the binary Al-1% Mn is 173 kJ/mol.[9] 3. Adding Fe in a proportion of 0.06 wt. % to the binary Al 1% Mn reduces the activation energy to 141 kJ/mol, and 4. The coefficients of diffusion of the main alloying agents Mn, Fe, and Si in Al given in Table II[10] indicate the capacity of these alloying agents to move in Al at the temperature range under study.

Table II. Diffusion coefficients of the main alloying agents in the AA3003 alloy in Al in units of ú²/sec.

Temperature (°C)	Mn	Fe	Si
127	$4.4x10^{-12}$	$8.9x10^{-1}$	$3.9x10^{-2}$
298	$5.9x10^{-3}$	$1.8x10^{2}$	$1.1x10^{4}$
394	7.9	$1.2x10^{3}$	$8.7x10^{5}$
441	$9.8x10^{1}$	$2.2x10^{3}$	$3.1x10^{6}$
496	$2.2x10^{3}$	$4.3x10^{3}$	$2.1x10^{7}$
560	$2.7x10^{4}$	$1.1x10^{4}$	$1.3x10^{8}$

Considering these premises, and knowing, in addition, that the intrinsic resistivities of Mn, Fe, and Si in Al in solid solution are 2.94, 2.56, and 1.02 μΩcm / wt. % and 0.34, 0.058, and 0.088 μΩcm / wt. % out of solid solution,[13] respectively, and that only a very small fraction of Fe is soluble in Al, we then can infer the following:

1. The behavior of the electrical resistivity in the first stage of aging is governed by the diffusion of Si, its effect being hardly perceptible due to the speed of the occurrence at higher temperatures. Between 350 °C and 450 °C the Fe atoms are more mobile than the Mn atoms but less so than the Si atoms, their resistivity being 2.5 times greater than that of the Si atoms, which induces us to think that for intermediate aging, both Si and Fe precipitate. The equilibrium phase in this temperature range, a-$(MnFe)_3SiAl_{12}$, reported in the literature,[9,12,13] is formed when Mn atoms are incorporated at the latter stage of aging. For temperatures above 450 °C the Si precipitates very quickly, thus making the Fe and the Mn compete to form the equilibrium phase $Al_6(Mn,Fe)$.
2. The kinetic study permits the confirmation of the assertions stated above. The kinetics represented by a power law both for N = 1/2 and N = 1/3 contemplates that at the onset of the precipitation for temperatures below 350°C, where the Si is the main participant, the activation energy is relatively low, 54 kJ/mol, whereas the involvement of both Fe and Mn in those early stages of precipitation requires activation energies of 128 kJ/mol or 145 kJ/mol depending on the Y range. The equilibrium phase at high temperatures and high Ys harmonizes with an N value of 1/3 and with a Q value of 162 kJ/mol. The three-dimensional diffusion model generates an elevated Y region with a 48 kJ/mol energy value for temperatures below 450 °C, whereas at higher temperatures Q has a value of 156 kJ/mol. These energies are thus in agreement with the values of the preceding model, the first one with a process of quick diffusion and the second one with the equilibrium phase $Al_6(Mn,Fe)$. The first- and second- order reaction models reflect, though at different ranges of Y, a situation similar to that observed in the three-dimensional diffusion model; that is, two processes limited by T = 450 °C, and whose energies of activation, in the ranges previously mentioned, basically reflect the participation of Si for low Ts and of Mn for high Ts. The JMA model is undoubtedly the one that shows a greater number of values different from N where K remains constant. In the case of P = 0, the exponent N = 1/3 foretells, for intermediate Y values, a process whose activation energy is 112 kJ/mol. For N = 1/2 this model reproduces the previously mentioned behavior for temperatures below and above 450°C and Q values of 68 kJ/mol and 155 kJ/mol respectively. For P = 1 and high Y values, the exponent N = 1 is also capable of signaling two processes, one below and one above 450 °C, with respective energies of 66 kJ/mol and 146 kJ/mol. Of the models studied, only the Fuyita-Damask one does not allow us to obtain a constant K zone for real values of P.

This analysis allows us to establish that, in general, all the reaction models have a Y range where they can be considered valid. As the Y range comprises the smallest transformation span, the difference that would result with the value obtained when we use nonlinear regression for this model, which is applicable along the whole length of Y, would be greater. This somehow justifies the method used in the present work.

CONCLUSION

We have used resistivity measurements to assess the validity of some reaction models to determine the real kinetic parameters associated with the transformation that occurs when an AA3003 alloy is aged at different temperatures. Our results allow us to conclude as follows:

1. There are well defined and reduced Y or aging-time regions where several of the models reviewed are valid; however, the attempt to encompass the whole extension of conversion or the whole Y range alters the value of the activation energy, thus creating the ambiguity reported in the literature.
2. The resistivity measurements show a sigmoid behavior both at 350 °C and at 550 °C, whereas at intermediate temperatures, the behavior appears to comprise two phases, the property decrease being associated with the structural transformation or precipitation that occurs during the aging process.
3. In light of the information we have regarding the alloying elements in AA3003, three processes of transformation are identified: The first is generally reported for low values of Y and for temperatures below 450 °C with an

energy close to 50 kJ/mol, where Si is the basic participant; the second is for intermediate Y values, characterized by N exponents different from those of the first case and by an activation energy in the neighborhood of 120 kJ/mol corresponding to the equilibrium phase at temperatures close to 350 °C or to the metastable phase reported at higher temperatures and identified in the literature[12] as α-$(MnFe)_3SiAl_{12}$. The third corresponds to the equilibrium phase at high Ts, identified as the $Al_6(Mn,Fe)$ phase and whose energy of activation is in the neighborhood of 155 kJ/mol[12].

The methodology of analysis proposed allows the validation of the parameters that pertain to the transformation itself and which are defined by particular models, as well as the rejection of those models that do not satisfy the premise stated at the beginning.

ACKNOWLEDGEMENTS

This work is supported by the Consejo de Investigación de la Universidad de Oriente under Project No CI. 5-1002-0938/00 UDO. I want to convey my appreciation to Carlos Mota and his company Traduce, C.A. for reviewing this manuscript.

REFERENCES

1. **Binder, K**., Statistical Mechanics of Nucleation and Phase Separation. *Proceedings of the IUPAP Conference on Statistical Physics*, Budapest, 1995, pp. 219-244.
2. **Budrugeac, P., Criado, J. M., Gotor, F. J., Popescu, C., Segal, E.,** Kinetic Analysis of Dissociation of Smithsonite from a set of Non-Isothermal Data Obtained at Different Heating Rates. *J. Thermal Anal.*, **63:** 777-786. 2001.
3. **Burke, J.,** *La cinétique des changements de phase dans les metaux*. Masson et Cie Éditeurs, Paris, 1968, p. 144.
4. **Cahn, J. W.,** On Spinodal Decomposition. *Acta Metall.*, **9:** 795-806. 1961.
5. **Christian, J. W.,** *The theory of transformations in metals and alloys. Part I*. Pergamon Press. Oxford, 1975, pp. 17-20, 542.
6. **Damask, A., Danielson, G., Dienes, G.,** A kinetic theory in dilute solid solutions: Application to the precipitation of carbon and nitrogen in ±-iron. *Acta Metall.*, **13:** 973-89. 1965.
7. **Flynn, J. H.,** The "Temperature Integral"- Its use and abuse. *Thermochim. Acta*. **300**: 83-92, 1997.
8. **Fujita, F. E.,** Ono Y., Inokuti Y., On the precipitation of carbon in super purity ±-iron. *Transaction ISIJ*. **6:** 363-371. 1968.
9. **Goel, D. B., Furrer, P., Warlimont, H.,** Precipitation characteristics of aluminium-manganese (cooper, iron) alloys. *Aluminium*. **50:** 511-16. 1974.
10. **Hatch, J. E**. Eds. ALUMINUM: Properties and Physical Metallurgy. ASM, Metals Park, OH, 1984, p. 140.
11. **Hillert, M.,** A Solid-Solution Model for Inhomogeneous Systems. *Acta Metall.*, **9:** 525-535. 1961.
12. **Luiggi, N**., Isothermal Precipitation of Commercial 3003 Al alloys Studied by Thermoelectric Power. *Metall. Mater. Trans. B.*, **28B:**125-133. 1997.
13. **Luiggi, N.,** Analysis of Thermoelectric Power Measurements in the Study of Precipitation Kinetics in 3003 Alloy. *Metall. Mater. Trans., B.* **28B**: 149-159. 1997.
14. **Luiggi, N., Betancourt, A.**, Kinetics of Simultaneous Two-Phase Precipitation in the Fe-C System. *Metall. Mater. Trans., B*. **28B:**161-168. 1997.
15. **Luiggi, N., Betancourt, A.,** Multiphase Precipitation of Carbides in Fe-C Systems: Part I. Model Based Upon Simple Kinetic Reactions. *Metall., Mater. Trans. B*. **25B:** 917-925. 1994.
16. **Mirold, P., Binder, K.,** Theory for the Initial Stages of Grain Growth and Unmixing Kinetics of Binary Alloys. *Acta Metall.*, **25:** 1435-1444. 1978.
17. **Vyazovkin, S., Wight, Ch.,** Isothermal and Nonisothermal Reaction Kinetics in Solids: In Search of Ways toward Consensus. *J. Phys. Chem. A.,* **101:** 8279-8284. 1997.

Correspondence: Ney José Luiggi Agreda.GFM, Dpto. de Física, Escuela de Ciencias, Núcleo de Sucre, Universidad de Oriente, Cumaná, Estado Sucre, Venezuela. Apdo. Postal 299. Postalddress: Código: 17 Apartado postal: 299 Cumaná Edo. Sucre VENEZUELA Fax: 58-0293-4302323.
Correo electrónico: nluiggi@sucre.edu.udo.ve